

# Characteristics of underwater lighting based on white LEDs

Zeyuan Qian<sup>a,†</sup>, Xugao Cui<sup>a,†</sup>, Zitong Wang<sup>a</sup>, Gufan Zhou<sup>a</sup>, Runze Lin<sup>a</sup>, Erdan Gu<sup>a,b</sup>, Pengfei Tian<sup>a,\*</sup>

<sup>a</sup> Institute for Electric Light Sources, School of Information Science and Technology, Fudan University, Shanghai 200438, China

<sup>b</sup> Institute of Photonics, Department of Physics, University of Strathclyde, Glasgow, United Kingdom

\* Corresponding author. E-mail address: pftian@fudan.edu.cn (P. Tian).

† These authors contributed equally to this work.

## ARTICLE INFO

Keywords:

Underwater white LED illumination

RGB-LED

PC-LED

CRI

Lambert-Beer model

Attenuation coefficient

## ABSTRACT

This work systematically analyzed the application of LEDs in underwater white lighting. The characteristics of a RGB-LED and a phosphor-converted LED (PC-LED) have been compared in different water types. The green light shows the smallest attenuation, while the red light has the greatest attenuation coefficient. Such different attenuation effects at different wavelengths lead to the different spectra, CIE coordinates and color rendering index (CRI) of the two kinds of LEDs. With increasing distance, the illuminance of the PC-LED decreases much more rapidly than the RGB-LED due to the stronger attenuation of the wide phosphor-based yellow spectrum. However, the CIE coordinates calculated from the spectra of the PC-LED vary little due to the wider yellow spectrum. On the contrary, the CIE coordinates shift is very clear for the RGB-LED. What's more, the CRI of the RGB-LED increases at distances from 0 to 1.5 m, and then decreases at longer distances, but the CRI of the PC-LED keeps decreasing at all distances, which can be explained by the variation of the R values of the color samples due to wavelength dependent light attenuation. This work will benefit the applications and designs of LED-based underwater lighting.

## 1. Introduction

In recent years, with the development of deep ocean exploitation and underwater Internet of Things (IOT), significant attention has been paid to underwater white light illumination. For example, it is required for divers and underwater robots to gain high-quality visual fields and high-quality images and videos [1,2]. With the rapid development of solid-state lighting (SSL), more and more underwater operations utilize SSL sources [3], owing to the high luminous efficiency and flexibility. In addition, underwater SSL can be combined with underwater wireless optical communication (UWOC) to realize potential underwater wireless networks and IOT, which is another advantage of solid-state light sources over traditional gas discharge sources in underwater lighting [4-8].

LED and laser diode (LD) have been applied in underwater white light illumination to increase underwater lighting distance due to high optical power density [9]. Speckle effect occurs when LD is directly used in lighting, which can obscure the observer's visual field or the captured image, unless employing designs like pulsed lasers to eliminate the coherence [10]. In addition, LD is unable to directly produce large-area lighting due to its high collimation, and diffusers are required for white light illumination [8]. These designs and techniques would complicate underwater laser lighting systems and increase costs. In comparison, LED is favored in practical underwater white illumination due to its advantages of low cost, high efficiency, and large lighting area [3]. Some underwater LED illuminations were reported [11-14], among which some detailed parameters, including the characteristics of large field of view of 70°, large area, long distance at up to 20 m [13], and high CRI over 70 [14] were presented. The Inherent Optical Properties (IOP) Theory with the Lambert-Beer underwater light transmission model was used to explain the propagation of light in water [15]. Nevertheless, the IOP theory presumes the condition of parallel and monochromatic incident light, which is not the case in most practical scenarios of underwater LED white light illumination using multicolor light with divergence angles. Further, the light-field average cosine method using Monte Carlo ray tracing was adopted [12,13,16], but the method did not describe chromaticity parameters. Chromaticity parameters, including CRI, spectra and chromaticity coordinates, are important to characterize the white light. CRI has been studied for underwater white LED illumination [14], but detailed underwater spectra and chromaticity coordinates still need more research.

In this work, a white PC-LED and a red, green and blue trichromatic white LED (RGB-LED) were adopted as light sources. We systematically studied various chromaticity parameters at different underwater distances in different water types experimentally and theoretically. We expect this work will help the development of underwater lighting based on white LEDs.

## 2. Experimental details

Based on the attenuation coefficients of 0.151 m<sup>-1</sup> and 0.398 m<sup>-1</sup> for water types of clear ocean water and coastal ocean water in the references [17-20], we estimated Maalox concentrations to simulate water types, which were 171.9 mg/m<sup>3</sup> and 699.8 mg/m<sup>3</sup>, respectively. Equation (1) can be used to calculate the underwater attenuation of light, as expressed by:

$$\frac{I(\lambda)}{I_0(\lambda)} = e^{-c(\lambda)d}, \quad (1)$$

where,  $c$ ,  $d$ , and  $\lambda$  represent the attenuation coefficient, the distance traveled by light in water, and the wavelength, respectively, and  $I_0$  and  $I$  are optical power, luminous flux or illuminance before and after attenuation, respectively.

We performed experiments of red, green, and blue light propagation through Maalox suspensions to study light attenuation in the simulated seawaters. The light source used for this experiment is a RGB-LED, in which the red, green, and blue LEDs can be driven separately to emit monochromatic light or driven simultaneously to emit white light. We packaged the commercial LED chips (Cree XB-D RED/GRN/BLU-2525) on an aluminum printed circuit board (PCB) in a common anode. The distance between each other is less than 1 mm. The voltages of the red, green, and blue LED are 2.08, 3.47, and 2.72 V, with the corresponding currents of 0.15, 0.24,

and 0.04 A, respectively. The illuminances of the red, green, and blue LED are 256, 687, and 21 lux, respectively, which is consistent with the relative vision function. Higher current and voltage of the green LED may come from lower efficiency and chip design. A Fresnel lens with a focal length of 10 cm was used to adjust the divergence angle and the underwater illumination area. In this experiment, we set the distance between the Fresnel lens and the LED to be 9.0 cm, and then measured the center illuminance of red, green and blue light by a Spectral Scintillation Illuminometer (Everfine SFIM-300, measurement accuracy  $\pm 3\%$ ) at varied distances in the 171.9 and 699.8 mg/m<sup>3</sup> Maalox suspensions. Fig. 1 shows the underwater white-lighting system, in which the light beam is scattered by the water with Maalox. The measured center illuminances versus underwater distance curves for the RGB-LED in separate driving mode are shown in Fig. 2. The illuminance decreases exponentially with increasing underwater distance, consistent with Equation (1).

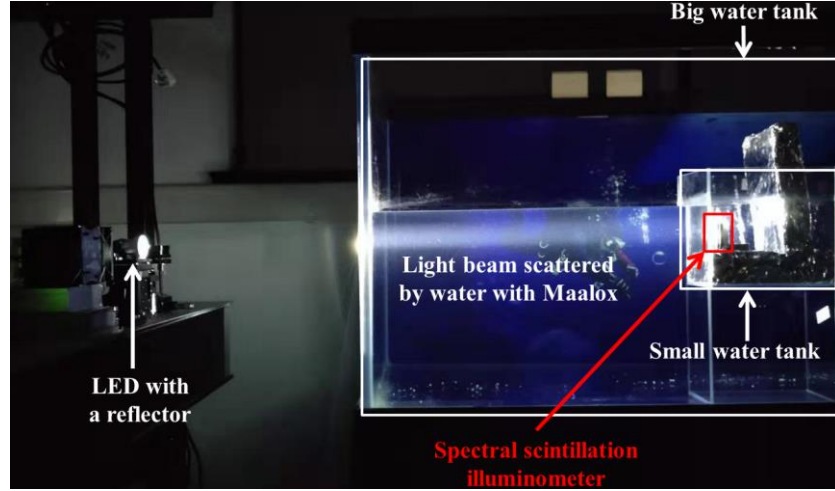


Fig. 1. Image of the LED white-light system for underwater lighting.

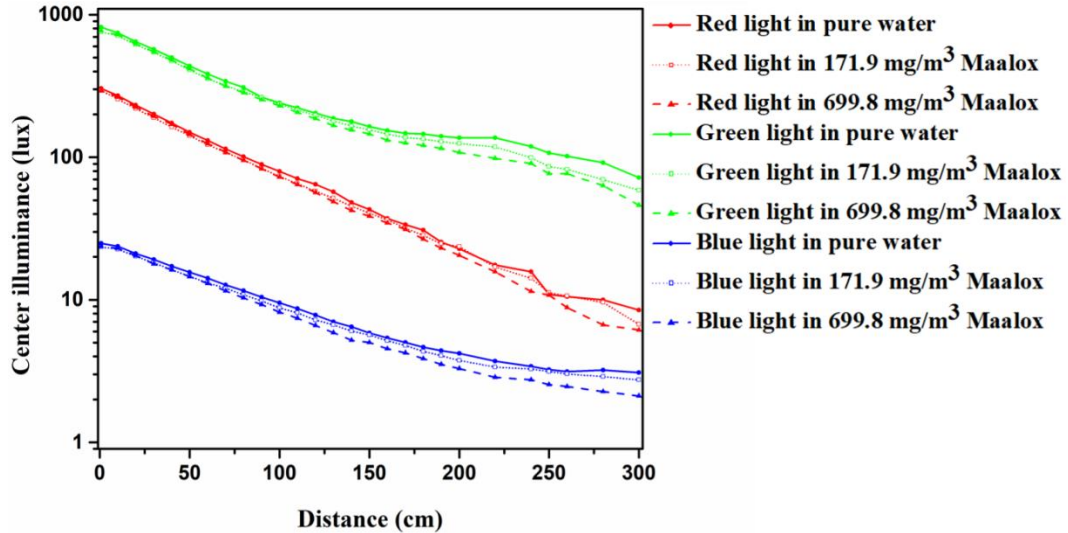


Fig. 2. Center illuminances of red, green and blue light at varied underwater distances in pure water and Maalox suspensions.

After fitting, the attenuation coefficients of the red, green and blue light in the pure water, 171.9 mg/m<sup>3</sup> Maalox and 699.8 mg/m<sup>3</sup> Maalox can be obtained, as shown in Table 1. We can find that the attenuation coefficient of the green light is the lowest, and the attenuation coefficient of red light is much higher than that of the green or the blue light. It has been reported that in the visible light range, the scattering coefficient of water decreases with increasing wavelength, while the absorption coefficient generally increases with increasing wavelength [20-22]. Considering the competitive mechanism of absorption and scattering, the lowest value of the water attenuation coefficient of green light in our experiment is reasonable [20,21]. If monochromatic light was applied in underwater lighting, the green light would be quite suitable. When RGB white light is applied in underwater lighting, the power of the red, green and blue LED needs to be adjusted according to varied underwater distances. As the water quality becomes turbid (from pure water to 699.8 mg/m<sup>3</sup> Maalox), the attenuation coefficient of the green or the blue light changes more than the red light.

After measuring the initial spectra of the red, green and blue LED, spectra of each LED at different distances in the pure water, 171.9 mg/m<sup>3</sup> Maalox and 699.8 mg/m<sup>3</sup> Maalox can be calculated according to Equation (1), and then summed to obtain the theoretical spectra of the white RGB-LED according to the equation:

$$P_k(\lambda, d) = P_R(\lambda)e^{-c_R d} + P_G(\lambda)e^{-c_G d} + P_B(\lambda)e^{-c_B d}, \quad (2)$$

where  $P_k$ ,  $P_R$ ,  $P_G$ , and  $P_B$  represent the theoretical spectra of the white RGB-LED, and the initial spectra of the red, green and blue LED, respectively;  $c_R$ ,  $c_G$ , and  $c_B$  represent the attenuation coefficients of the red, green and blue light, respectively. Thus, the theoretical CRI values of the white RGB-LED at different distances in the pure water, 171.9 mg/m<sup>3</sup> Maalox and 699.8 mg/m<sup>3</sup> Maalox can be calculated to explain the experimental results.

**Table 1**

Calculated attenuation coefficients of red, green and blue light in pure water and Maalox suspensions.

Water type	Attenuation coefficient of different colors (m <sup>-1</sup> )		
	Red(623nm)	Green(523nm)	Blue(450nm)
Pure water	0.72	0.24	0.25
171.9 mg/m <sup>3</sup> Maalox	0.73	0.26	0.29
699.8 mg/m <sup>3</sup> Maalox	0.76	0.35	0.36

We also measured the performance of the most common PC-LED using blue light to excite yellow Yttrium Aluminum Garnet (YAG) phosphors. The PC-LED with correlated color temperature (CCT) over 7000 K was commercially available (Cree XPE Q5). We packaged it on a reflector, and the heat was dissipated through a heat sink and a cooling fan. The CCT of the PC-LED is similar to the RGB-LED's (over 6000 K), making the experimental results more comparable. The experimental setup of the PC-LED underwater illumination system is similar to the RGB-LED system described above.

By adjusting the optical designs of the PC-LED and the RGB-LED including the position of the Fresnel lens and the diameter of the reflector, varied underwater illumination beams with certain aperture angles were generated. Under such conditions, a spectral scintillation illuminometer was used to measure the center illuminance, underwater spectrum, chromaticity, CCT, and CRI.

### 3. Results and discussion

The R, G, and B curves in Fig. 2 of the RGB LEDs for each type of water were summed, and the results were shown in Fig. 3(a) with aims of being compared with the center illuminance versus underwater distance curves in Fig. 3(b) of the PC-LED in the pure water and Maalox suspensions. For both the RGB-LED and the PC-LED, the higher Maalox concentration leads to stronger attenuation of light and the center illuminances decrease with increasing distance in the three types of water. In addition, the slope in Fig. 3(b) is larger than that in Fig. 3(a), indicating that the white light of the PC-LED is attenuated much more severely than the RGB-LED. The reason is that the yellow spectrum of the PC-LED covers wider wavelength range from 489 nm to 780 nm, among which the long-wavelength light suffers stronger attenuation.

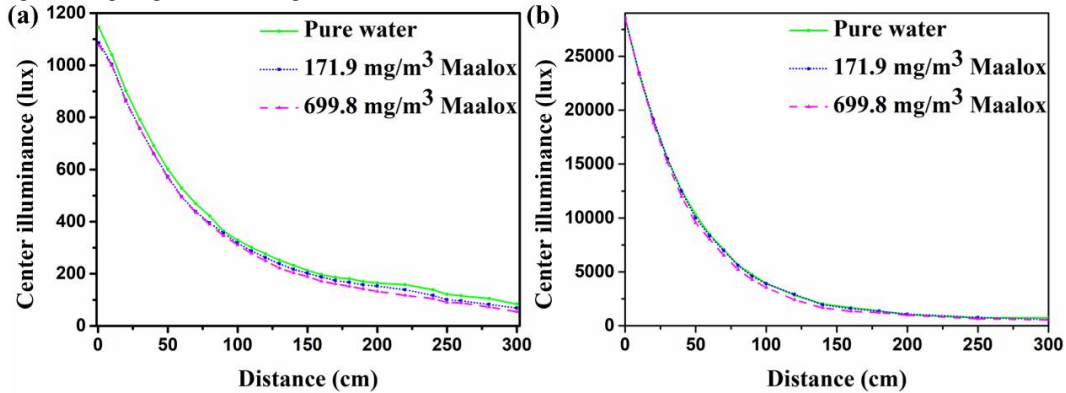


**Fig. 3.** Center illuminances of (a) the RGB-LED and (b) the PC-LED at varied underwater distances in pure water and Maalox suspensions.

The light decay effects can be also illustrated in terms of spectra in Fig. 4 which shows normalized spectra of the RGB-LED and the PC-LED at varied underwater distances in 699.8 mg/m<sup>3</sup> Maalox. In the figure, green light with the smallest attenuation ratio is normalized. For each LED, it is clear that the normalized intensities of both shorter and longer wavelength light gradually decrease as the underwater distance increases, which can be explained by the different attenuation coefficients in Table 1.

The chromaticities of the underwater RGB-LED and the PC-LED are shown in Fig. 5(a) and (b), respectively. In both Fig. 5(a) and (b), the chromaticity coordinates drift to the green color region with increasing underwater distance. However, the chromaticity coordinates of the PC-LED drift much less than the RGB-LED with increasing underwater distance, owing to the wider yellow spectra of the PC-LED and the rapid attenuation of red and blue spectra of the RGB-LED, which is an advantage of the PC-LED as an underwater white light source. When the RGB-LED is applied in underwater lighting, large color drift happens with the change of the underwater distance. However, we can adjust light colors conveniently, and thus can generate white light with required color coordinates at varied underwater distances with the RGB-LED. Furthermore, from Fig. 5(a) and (b) we can also obtain CCT change through the red arrow curve of color coordinates and the blackbody radiance curves in black, at the distances from 0.7 cm to 3 m. The CCTs of the RGB-LED and the PC-LED are changed from 6056 K to 12043 K and from 7060 K to 8387 K, respectively. The CCT of the

the PC-LED is changed much less than the RGB-LED with increasing underwater distance, which can also owe to the color stability discussed above.

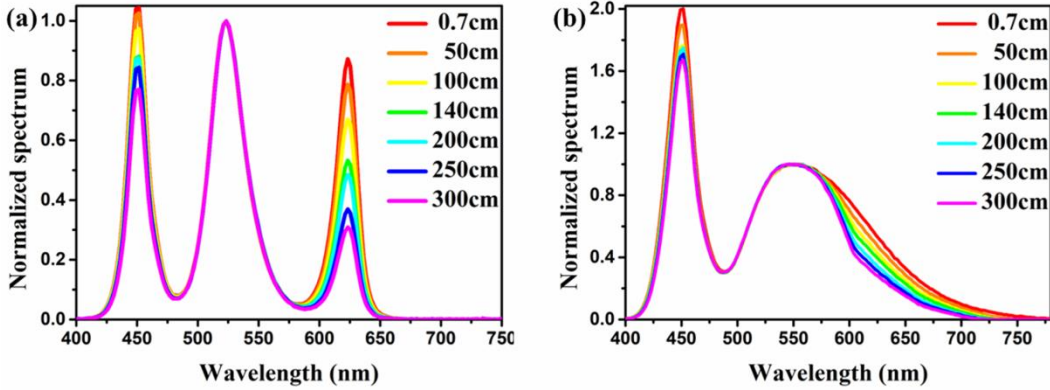


Fig. 4. Normalized spectra of (a) the RGB-LED and (b) the PC-LED at varied underwater distances in the 699.8 mg/m<sup>3</sup> Maalox.

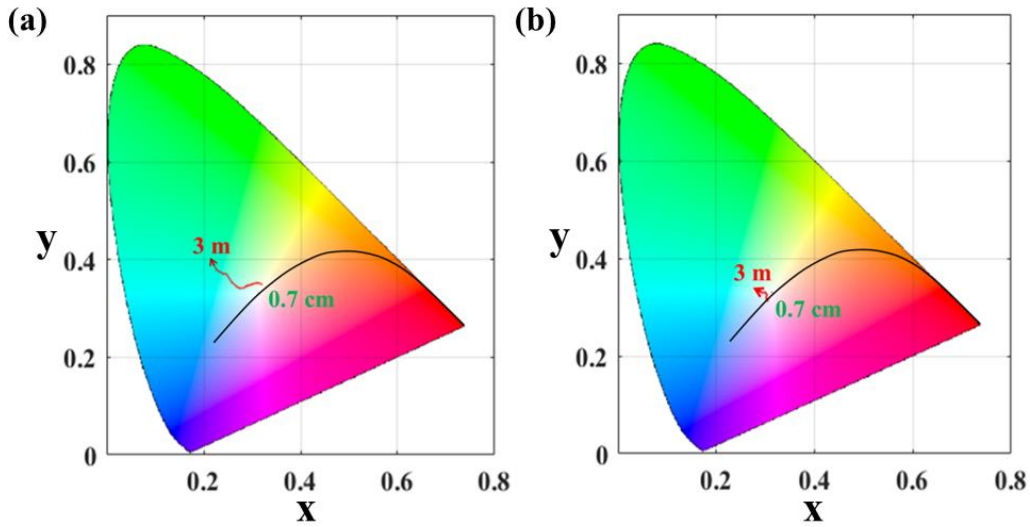


Fig. 5. CIE 1931 coordinates of (a) the RGB-LED and (b) the PC-LED at varied underwater distances in the 699.8 mg/m<sup>3</sup> Maalox. The direction of the arrow indicates the direction in which underwater distance increases.

The CRI versus underwater distance curves of the RGB-LED and the PC-LED in the pure water, 171.9 mg/m<sup>3</sup> Maalox and 699.8 mg/m<sup>3</sup> Maalox are shown in Fig. 6(a) and (b), respectively. It is clear that CRI for different water types shows little difference at varied distances, except the divergence of CRI in Fig. 6(a) at distances longer than 180 cm may come from the spatially separation of RGB LEDs. What's more, from Fig. 6(a), the CRI increases with increasing the underwater distance to about 1.5 m, and then declines with longer underwater distances. However, from Fig. 6(b), the CRI keeps decreasing with increasing distance. Furthermore, the PC-LED has higher CRI values at distances less than 70 cm compared with the RGB-LED. CRI is defined by the equation:  $CRI (R_a) = \sum_{i=1}^8 R_i / 8 = 100 - \sum_{i=1}^8 \Delta E_i / 8$ , where  $R_i$  and  $\Delta E_i$  represent the color rendering index for the color sample  $i$ , and the color difference of the color sample  $i$  when using the light source under test and the reference light source, respectively [23]. In general, to gain a high  $R_a$ , a high light intensity and a broad spectrum of yellow-green light are required. However, the RGB-LED in this work has a relatively narrow green spectrum, so the initial  $R_a$  of the RGB-LED is quite low (lower than 50). As the distance increases, due to the increasing attenuation of blue and red light, the proportion of green light intensity increases, so  $R_a$  rises and the sum of other  $R_i$  decreases. At distances from 0 to 1.5 m, the increase of  $R_a$  is larger than the sum of the decrease of other  $R_i$ . Thus, the CRI of the RGB-LED increases at smaller distances. Different from the RGB-LED, the PC-LED has a broad spectrum of yellow-green light. So the PC-LED has a high initial  $R_a$ , resulting in the higher CRI values at distances less than 70 cm compared with the RGB-LED. As the distance further increases, the decrease of the sum of  $R_i$  leads to the decrease in CRI for the PC-LED, which is the same reason for the CRI decrease of the RGB-LED at longer distances.

#### 4. Conclusion

In this study, we explored experimentally and analyzed systematically the underwater white light illumination of the RGB-LED and the PC-LED in different water types. The PC-LED has greater illuminance decrease and better color stability, i.e. smaller change of chromaticity coordinates, CCT and CRI with the increase of the underwater distance. The RGB-LED has advantage of conveniently adjusting certain light colors. Our work can provide helps in optimizing the white light characteristics in underwater LED lighting applications.

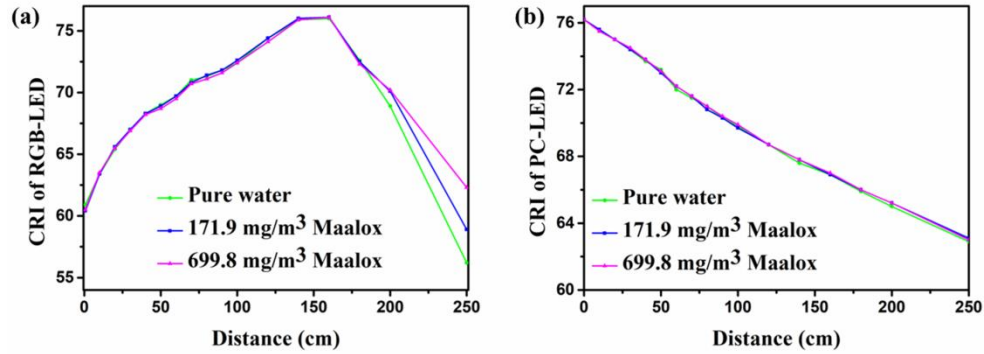


Fig. 6. CRI of (a) the RGB-LED and (b) the PC-LED at varied underwater distances in pure water and various Maalox suspensions.

### Declaration of Competing Interest

The authors declare that they have no known competing financial interests or personal relationships that could have appeared to influence the work reported in this paper.

### Acknowledgment

This work was supported by National Natural Science Foundation of China (NSFC) (No. 61974031), National Key Research and Development Program of China (No. 2021YFE0105300) and Fudan University-CIOMP Joint Fund (No. FC2020-001).

### References

- [1] Y. Liu, H. Xu, D. Shang, C. Li, X. Quan, An underwater image enhancement method for different illumination conditions based on color tone correction and fusion-based descattering, *Sens.* 19 (2019) 5567.
- [2] M.S. Baskoro, B. Murdiyanto, Zulkarnain, T. Arimoto, The effect of underwater illumination pattern on the catch of bagan with electric generator in the west Sumatera sea waters, Indonesia, *Fisheries Sci.* 68 (2002) 1873-1876.
- [3] K.R. Hardy, M.S. Olsson, B.P. Lakin, K.A. Steeves, J.R. Sanderson, J.E. Simmons, P.A. Weber, Advances in high brightness light emitting diodes in underwater applications, *Oceans 2008*, Quebec, 2008.
- [4] P. Tian, X. Liu, S. Yi, Y. Huang, S. Zhang, X. Zhou, L. Hu, L. Zheng, R. Liu, High-speed underwater optical wireless communication using a blue GaN-based micro-LED, *Opt. Express* 25 (2017) 1193-1201.
- [5] X. Liu, S. Yi, X. Zhou, Z. Fang, Z. Qiu, L. Hu, C. Cong, L. Zheng, R. Liu, P. Tian, 34.5 m underwater optical wireless communication with 2.70 Gbps data rate based on a green laser diode with NRZ-OOK modulation, *Opt. Express* 25 (2017) 27937-27947.
- [6] H. Chen, X. Chen, J. Lu, X. Liu, J. Shi, L. Zheng, R. Liu, X. Zhou, P. Tian, Toward long-distance underwater wireless optical communication based on a high-sensitivity single photon avalanche diode, *IEEE Photon. J.* 12 (2020) 1-10.
- [7] S. Zhu, X. Chen, X. Liu, G. Zhang, P. Tian, Recent progress in and perspectives of underwater wireless optical communication, *Prog. Quant. Electron.* 73 (2020) 100274.
- [8] X. Liu, S. Yi, X. Zhou, S. Zhang, Z. Fang, Z. Qiu, L. Hu, C. Cong, L. Zheng, R. Liu, P. Tian, Laser-based white-light source for high-speed underwater wireless optical communication and high-efficiency underwater solid-state lighting, *Opt. Express* 26 (2018) 19259-19274.
- [9] S. Tetlow, R.L. Allwood, Development and applications of a novel underwater laser illumination system, *Underwater Technol.* 21 (1995) 13-20.
- [10] J.W. Goodman, *Speckle phenomena in optics: theory and applications*, Roberts and Company Publishers, Greenwood Village, 2007, pp. 165-197.
- [11] M.S. Olsson, K.R. Hardy, J.R. Sanderson, Underwater application of high-power light emitting diodes, *Sea Technol.* 48 (2007) 31-34.
- [12] E.M. Gutsait, Analysis of the illuminance provided by LED modules placed at large distances from illuminated objects, *J. Commun. Technol. El.* 54 (2009) 107-118.
- [13] S.C. Shen, H.J. Huang, C.C. Chao, M.C. Huang, Design and analysis of a high-intensity LED lighting module for underwater illumination, *Appl. Ocean Res.* 39 (2013) 89-96.
- [14] M.H. Lai, C. Hung, Study on improvement of CRI using RGB LED lights for underwater environments, *Optik* 129 (2017) 30-34.
- [15] C.H. Chang, C.C. Liu, C.G. Wen, Integrating semianalytical and genetic algorithms to retrieve the constituents of water bodies from remote sensing of ocean color, *Opt. Express* 15 (2007) 252-265.
- [16] E.M. Gutsait, Analysis of LED modules for local illumination, *J. Commun. Technol. El.* 52 (2007) 1377-1395.
- [17] F. Hanson, S. Radic, High bandwidth underwater optical communication, *Appl. Optics* 47 (2008) 277-283.
- [18] B.M. Cochenour, L.J. Mullen, A.E. Laux, Characterization of the beam-spread function for underwater wireless optical communications links, *IEEE J. Oceanic Eng.* 33 (2008) 513-521.
- [19] P. Tian, H. Chen, P. Wang, X. Liu, X. Chen, G. Zhou, S. Zhang, J. Lu, P. Qiu, Z. Qian, X. Zhou, Z. Fang, L. Zheng, R. Liu, X. Cui, Absorption and scattering effects of Maalox, chlorophyll, and sea salt on a micro-LED-based underwater wireless optical communication, *Chin. Opt. Lett.* 17 (2019) 100010.
- [20] Z. Zeng, S. Fu, H. Zhang, Y. Dong, J. Cheng, A survey of underwater optical wireless communications, *IEEE Commun. Surv. Tut.* 19 (2016) 204-238.
- [21] J.A. Simpson, A 1 Mbps underwater communications system using LEDs and photodiodes with signal processing capability, M.S. thesis, Dept. Elect. Eng., North Carolina State Univ., Raleigh, NC, USA, 2007.
- [22] R.M. Pope, E.S. Fry, Absorption spectrum (380-700 nm) of pure water. II. Integrating cavity measurements, *Appl. Optics* 36 (1997), 8710-8723.
- [23] H. Xu, Sample-independent color rendering index, *Color Res. Appl.* 20 (2010) 251-254.